EFFECTS OF NON-ORTHOGONAL BOUNDARY FITTED GRIDS IN THE SOLUTION OF TWO-PHASE FLOW IN PETROLEUM RESERVOIR SIMULATION

Brauner Gonçalves Coutinho
Federal University of Campina Grande, Technology and Sciences Center, Departament of Mechanical Engineering
Av. Aprígio Veloso, 882, Bodocongó, PO Box 10069, CEP 58109-970, Campina Grande-PB, Brazil.
braunergc@yahoo.com

Francisco Marcondes
Federal University of Ceará, Technology Center, Mechanical and Industrial Engineering Department
Campus do Pici, PO Box 12144, CEP 60455-760, Fortaleza-CE, Brazil.
marconde@dem.ufc.br

Antonio Gilson Barbosa de Lima
Federal University of Campina Grande, Technology and Sciences Center, Departament of Mechanical Engineering
Av. Aprígio Veloso, 882, Bodocongó, PO Box 10069, CEP 58109-970, Campina Grande-PB, Brazil.
gilson@dem.ufpb.br

Abstract. Efficient mathematical models can be used to preview the behavior of the fluids present in the reservoir under several operation conditions. The main goal of this study is to obtain a numeric solution for two-phase problems with complex geometry reservoirs, through the finite-volume method in boundary-fitted coordinates. The physical model adopted is the standard black-oil, simplified to an immiscible, two-phase (oil-water) flow. It can be applied for studies in reservoirs for heavy oils without volatile hydrocarbons. The mass conservation equations, written in the mass fractions formulation, are solved using a fully implicit methodology and the Newton's method. In spite of computational time consumption, the great advantage of this methodology is the possibility to use larger time steps. The UDS scheme is used to evaluate the phase motilities in each control volume face. Attention will be given to the Jacobian matrix construction. The results are presented in terms of Newton's and solver iterations, CPU time used for build the Jacobian matrix and to solve the linear systems and for the whole simulations.

Keywords. Reservoirs simulation, finite-volume, black-oil, boundary-fitted coordinates.

1. Introduction

Before investing a new petroliferous basin, the exploration industry needs to know parameters that assure its commercial viability. If the financial return will not be guaranteed, the high costs involved in the implantation of exploration structures become a risky transaction. Generally, when a reservoir starts operate, the high pressures below the earth's surface are enough to drive the flow up to wells. As time goes on, pressures became equal in all positions inside rock pores and some recoverable oil keeps into reservoir, unable to flow. An artificial mechanism becomes necessary to restore the pressure gradient in a process so-called Secondary Recovery. Even when the oil production from a reservoir starts to decrease, the field engineer may decide to increase the flow by injecting water into the reservoir. Water enters by injection wells and moves some of the remaining oil in the rock toward producing wells in the same reservoir. The producing wells then pump up the oil, water and gas. It is normal to use several injection wells surround each producing well. This method is so-called water flooding. Water flooding is the least expensive and most widely used secondary recovery method.

The study of oil reservoirs using laboratory experiments is a complex task. The confident reproduction of all fluid and rock conditions (temperature, pressure, geometry, composition) in the surface is almost impossible, or economically difficult.

In the petroleum industry, simulation may be used to predict the behavior of fluids inside a reservoir under different operation conditions. The physical problem may be simulated through reservoir simulation and studied including porous media (rock where the flow occurs), reservoir fluids (water, oil and gas), as well as the geometries of the impermeable borders. Major influence variables in the reservoir's useful life can also be studied, such as: composition, flow rate, characteristics of the injection fluid; correct location of injector and producing wells and changes of these positions according to the most current conditions of fluids saturations inside reservoir.

This study shows a numeric solution for complex geometry reservoirs, using the finite-volume method in boundary-fitted coordinates. UDS (Upstream Differencing Scheme) is used to evaluate the phase motilities in each control volume face. Mass conservation equations, written in the mass fractions formulation are solved using a fully implicit methodology and the Newton's method. In spite of computational time consumption, the great advantage of this methodology is the possibility to use larger time steps, Marcondes (1996).

The major issue of this paper, from the numerical point of view, is to illustrate the solver performance in the Newton method solution using Jacobian matrices constructed by five-points and nine-points schemes, considering parameters such as: Newton's and solver iterations; CPU time used for built the Jacobian matrix, solved the arising linear systems and for the whole simulations. Details about both schemes will be given afterwards.

2. Mathematical modelling

The standard black-oil is a mathematical model that can be used in reservoirs with heavy or low volatility hydrocarbons. It is an isothermal model where the behavior among the phases is governed by pressure and volume relationships. The characteristics of the model are:

- There are three components (water, oil and gas) and three phases (water, oil and gas);
- Water and oil phases neither mix nor interphase mass transfer;
- The gas component is dissolved in oil phase;
- Water and oil components cannot be found in the gas phase.

In the present study, a two-phase (oil-water) immiscible flow was considered. Neglecting the gravitational and capillarity effects, mass conservation equation for a generic phase p is given by

$$\frac{\partial}{\partial t}\left[\phi\rho^m Z^p\right] = \nabla.\left[\tilde{\lambda}^p \nabla P\right] - \tilde{m}^p \tag{1}$$

where the superscript p indicates the phase p, ϕ is the porosity, ρ^m is the average density of the mixture, Z is the mass fraction, P is the reservoir pressure, $\tilde{m}^p$ is the mass flow per unit of volume of the reservoir and $\tilde{\lambda}^p$ is the phase motility, defined as follows

$$\lambda^p = \frac{\rho^p \mathbf{k} k^{rp}}{\mu^p} \tag{2}$$

In Eq. (2), $\mathbf{k}$ is the absolute permeability, k^{rp} is the relative permeability, ρ^p is the density and μ^p is the viscosity of phase p.

Writing Eq. (1) for the oil and water phases, there are three unknowns (Z^o, Z^w and P) and two equations. The equation needed for the solution comes from global mass conservation, is given by,

$$Z^w + Z^o = 1 \tag{3}$$

More details of the Black-oil formulation in terms of mass fractions can be found in (Prais and Campagnolo,1991 and Cunha, 1996).

3. Numerical solution

Due to nonlinearities present in the governing equations, specially that one in the phase mobility, those equations do not have analytical solution. A numerical solution, such as finite-volume method, can be an alternative to this problem.

The main advantages of cartesian grids are the simplicity of the conservation balances and the easy solution of the resulting linear systems. The disadvantages are: difficulty to model complex geometries reservoirs, geologic faults, complex distribution of wells and grid orientation effect, Todd et all (1972). Non-orthogonal boundary fitted grids can turn the numerical method flexible to treat reservoirs with more complex geometries (Maliska, 1995; Cunha et all 1994).

3.1. Transformation of the governing equations

Considering only 2D problems Eq. (1) can be written for boundary fitted coordinates as,

$$\frac{1}{J}\frac{\partial}{\partial t}\left(\phi\rho^m Z^p\right) + \frac{\tilde{m}^p}{J} = \frac{\partial}{\partial\xi}\left[D_1^p\frac{\partial P}{\partial\xi} + D_2^p\frac{\partial P}{\partial\eta}\right] + \frac{\partial}{\partial\eta}\left[D_2^p\frac{\partial P}{\partial\xi} + D_3^p\frac{\partial P}{\partial\eta}\right] \tag{4}$$

where the coefficients D_i^p are given by

$$D_1^p = \frac{\tilde{\lambda}^p}{J}\left(\xi_x^2 + \xi_y^2\right); \quad D_2^p = \frac{\tilde{\lambda}^p}{J}\left(\xi_x\eta_x + \xi_y\eta_y\right); \quad D_3^p = \frac{\tilde{\lambda}^p}{J}\left(\eta_x^2 + \eta_y^2\right) \tag{5 a-c}$$

Equation (5 a-c) have all grid information, Maliska (1995).

3.2. Integration of the governing equations

Integrating Eq. (4) in space and in time for the volume shown on Fig. (1), the following equation is obtained

$$\frac{\Delta V}{J}\left[\left(\phi\rho^m Z^p\right)_P - \left(\phi\rho^m Z^p\right)_P^o\right] + \frac{\tilde{m}^p}{J}\Delta V\Delta t = \left[\left(D_1^p\frac{\partial P}{\partial \xi} + D_2^p\frac{\partial P}{\partial \eta}\right)_e - \left(D_1^p\frac{\partial P}{\partial \xi} + D_2^p\frac{\partial P}{\partial \eta}\right)_w\right]\Delta\eta\Delta\gamma\Delta t +$$

$$\left[\left(D_2^p\frac{\partial P}{\partial \xi} + D_3^p\frac{\partial P}{\partial \eta}\right)_n - \left(D_2^p\frac{\partial P}{\partial \xi} + D_3^p\frac{\partial P}{\partial \eta}\right)_s\right]\Delta\xi\Delta\gamma\Delta t \qquad (6)$$

where $\Delta V = \Delta\xi\Delta\eta\Delta\gamma$ is the volume dimensions on generalized coordinates system.
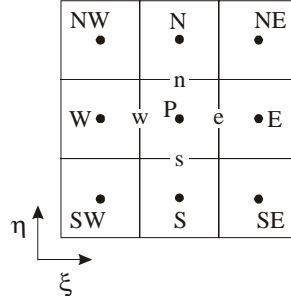
Figure 1 – Infinitesimal volume.

All differentials terms in right hand side of Eq. (6) are approached by central differencing scheme. The pressure gradients in the east face, for example, are given by,

$$\left(\frac{\partial P}{\partial \xi}\right)_e = \frac{P_E - P_P}{\Delta\xi} \qquad \left(\frac{\partial P}{\partial \eta}\right)_e = \frac{P_N + P_{NE} - P_S - P_{SE}}{4\Delta\eta} \qquad (7)$$

To evaluate the phase mobility in each control volume face it was employed the Upwind Differencing Scheme. Using again the east face λ^p is given by,

$$\tilde{\lambda}_e^p = \tilde{\lambda}_P^p \text{ if } \overline{u}_e^p > 0, \text{ and } \tilde{\lambda}_e^p = \tilde{\lambda}_E^p \text{ otherwise.} \qquad (8)$$

3.3. Fully implicit methodology

In this methodology the unknowns P and Z^o are implicitly calculated at the current time step. The equations are linearized by Newton's method. Passing to the left side all terms of Eq. (6) the following residual equation is obtained:

$$F_P^p = \frac{\Delta V}{J}\left[\left(\phi\rho^m Z^p\right)_P - \left(\phi\rho^m Z^p\right)_P^o\right] + \frac{\tilde{m}^p}{J}\Delta V\Delta t - \left[\left(D_1^p\frac{\partial P}{\partial \xi} + D_2^p\frac{\partial P}{\partial \eta}\right)_e - \left(D_1^p\frac{\partial P}{\partial \xi} + D_2^p\frac{\partial P}{\partial \eta}\right)_w\right]\Delta\eta\Delta\gamma\Delta t -$$

$$\left[\left(D_2^p\frac{\partial P}{\partial \xi} + D_3^p\frac{\partial P}{\partial \eta}\right)_n - \left(D_2^p\frac{\partial P}{\partial \xi} + D_3^p\frac{\partial P}{\partial \eta}\right)_s\right]\Delta\xi\Delta\gamma\Delta t \qquad (9)$$

Expanding this expression in Taylor's series, we have

$$\left(F_P^p\right)^{k+1} = \left(F_P^p\right)^k + \sum_{\forall X}\left(\frac{\partial F_P^p}{\partial X}\right)^k \Delta X = 0 \qquad (10)$$

where k is the iteration level and X represents the unknowns P and Z^o.

In the Newton's method, the solution in every time step is given when the residues tend to zero. Therefore, Eq. (10) in the short form is given by:

$$-F^k = \sum_{\forall X}\left(\frac{\partial F}{\partial X}\right)^k \Delta X \qquad (11)$$

In the matrix form, Eq. (11) can be written by:

$$A\Delta X = -F \tag{12}$$

where **A** is the Jacobian matrix of the residual function F on the k-th iteration.

The solution of the linear system, Eq. (12), allows calculating the P and Z^o values till the mass conservation in each time step is obtain. The Jacobian matrix **A** is a block matrix, i.e., all its elements are square matrices.

3.3.1. Nine points scheme

On this scheme, all neighboring points are considered on differentiation of the residual functions. Using this scheme, Eq. (11) will be given by

$$
\begin{aligned}
&\left(\frac{\partial F_P^p}{\partial P_P}\right)\Delta P_P + \left(\frac{\partial F_P^p}{\partial Z_P^o}\right)\Delta Z_P^o + \left(\frac{\partial F_P^p}{\partial P_W}\right)\Delta P_W + \left(\frac{\partial F_P^p}{\partial Z_W^o}\right)\Delta Z_W^o + \left(\frac{\partial F_P^p}{\partial P_E}\right)\Delta P_E + \left(\frac{\partial F_P^p}{\partial Z_E^o}\right)\Delta Z_E^o + \\
&\left(\frac{\partial F_P^p}{\partial P_S}\right)\Delta P_S + \left(\frac{\partial F_P^p}{\partial Z_S^o}\right)\Delta Z_S^o + \left(\frac{\partial F_P^p}{\partial P_N}\right)\Delta P_N + \left(\frac{\partial F_P^p}{\partial Z_N^o}\right)\Delta Z_N^o + \left(\frac{\partial F_P^p}{\partial P_{SW}}\right)\Delta P_{SW} + \left(\frac{\partial F_P^p}{\partial Z_{SW}^o}\right)\Delta Z_{SW}^o + \\
&\left(\frac{\partial F_P^p}{\partial P_{SE}}\right)\Delta P_{SE} + \left(\frac{\partial F_P^p}{\partial Z_{SE}^o}\right)\Delta Z_{SE}^o + \left(\frac{\partial F_P^p}{\partial P_{NW}}\right)\Delta P_{NW} + \left(\frac{\partial F_P^p}{\partial Z_{NW}^o}\right)\Delta Z_{NW}^o + \left(\frac{\partial F_P^p}{\partial P_{NE}}\right)\Delta P_{NE} + \left(\frac{\partial F_P^p}{\partial Z_{NE}^o}\right)\Delta Z_{NE}^o = -F_P^p
\end{aligned} \tag{13}
$$

3.3.2. Five points scheme

According to Cunha (1996), to simplify the linear system, the derivatives of the cross terms (SW, SE, NW, NE) may be considered only in the residual function. This procedure avoids additional terms in the Jacobian matrix when the coordinates lines are non-orthogonal. Using this scheme, the Eq. (11) can be rewritten as follows

$$
\begin{aligned}
&\left(\frac{\partial F_P^p}{\partial P_P}\right)\Delta P_P + \left(\frac{\partial F_P^p}{\partial Z_P^o}\right)\Delta Z_P^o + \left(\frac{\partial F_P^p}{\partial P_W}\right)\Delta P_W + \left(\frac{\partial F_P^p}{\partial Z_W^o}\right)\Delta Z_W^o + \left(\frac{\partial F_P^p}{\partial P_E}\right)\Delta P_E + \left(\frac{\partial F_P^p}{\partial Z_E^o}\right)\Delta Z_E^o + \\
&\left(\frac{\partial F_P^p}{\partial P_S}\right)\Delta P_S + \left(\frac{\partial F_P^p}{\partial Z_S^o}\right)\Delta Z_S^o + \left(\frac{\partial F_P^p}{\partial P_N}\right)\Delta P_N + \left(\frac{\partial F_P^p}{\partial Z_N^o}\right)\Delta Z_N^o = -F_P^p
\end{aligned} \tag{14}
$$

This approach simplifies the resultant linear system but it can either slow down the convergence rate or hamper the convergence if the mesh is highly non-orthogonal. In the results section of this work, some comparisons between both schemes will be shown and analyzed. More details about whole mathematical formulation can be found in (Cunha, 1996 and Coutinho, 2002).

4. Results

The example selected to evaluate the behavior of the approaches just mentioned in the last section was originally proposed by Hirasaki and O´dell (1970) and after studied by (Hegre et all,1986; Czesnat, 1998). They considered a reservoir with two producing wells equidistant from an injection well, as shown in Fig. (2). To investigate the grid effects they compared the volumetric production rate of each producing well. The mesh is aligned with the line that connects one producing-injector well and is diagonal to another pair, as shown in Fig. (3).
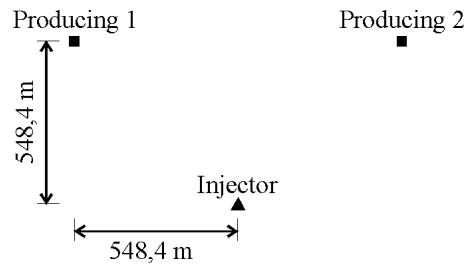
Figure 2 – Wells positions.
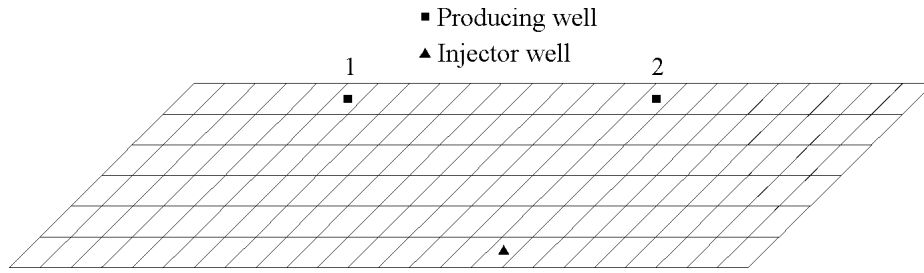
Figure 3 – Grid 24x6 volumes with 45° inclination.

For comparisons, meshes with 24 x 6 volumes were used, Fig. (3), and another with 48 x 20 volumes. Table (1) gives the relative permeabilities of the phases and Table (2) shows characteristic data of fluids and reservoir used in this work. Figure (4) presents saturation fields, in the elapsed time of 500 and 2000 days. Note that mesh with less number of volumes have generated results with high grid effects and numeric dispersion too. The injected water reaches the producing well 1 (aligned with the grid) faster than producing well 2. Considering that each producing well is equidistant to the injector well, physically, this phenomenon couldn't occur. This undesirable problem causes errors in water irruption time on producing wells. To investigate grid effects on reservoir simulation, many researches are being done in present day (Marcondes, 1996 and Czesnat 1998).

Table 1 – Relative permeabilities of the phases. Source: Hegre et all (1986).

S^w	k_{rw}	k_{ro}
0,25	0	0,92
0,3	0,02	0,705
0,4	0,055	0,42
0,5	0,1	0,24
0,6	0,145	0,11
0,7	0,2	0

Table 2 – Fluids and reservoir data. Source: Hegre et all (1986).

Porosity	$\phi = 0,19$	Residual oil saturation	$S_r^o = 0,2$
Permeability	$k = 0,049.10^{-12}$ m^2	Phases density	$\rho^w = \rho^o = 1000$ kg/m^3
Height	$h = 18,3$ m	Water reference volumetric formation factor	$B_{ref}^w = 1$ on P_{ref}
Initial pressure	$P_i = 27248.10^3$ Pa	Oil reference volumetric formation factor	$B_{ref}^o = 0,96$ on P_{ref}
Rock compressibility	$c^r = 0$ Pa^{-1}	Reference pressure	$P_{ref} = 27248.10^3$ Pa
Oil compressibility	$c^o = 1,45.10^{-9}$ Pa^{-1}	Water viscosity	$\mu^w = 0,5.10^{-3}$ Pa.s
Water compressibility	$c^w = 0,44.10^{-9}$ Pa^{-1}	Oil viscosity	$\mu^o = 2,0.10^{-3}$ Pa.s
Well radius	$r^w = 0,122$ m	Injection rate	$q_{inj} = 302,1$ m^3/dia
Initial water saturation	$S_i^w = 0,2$	Producing rate	$q_{prod} = 159$ m^3/dia
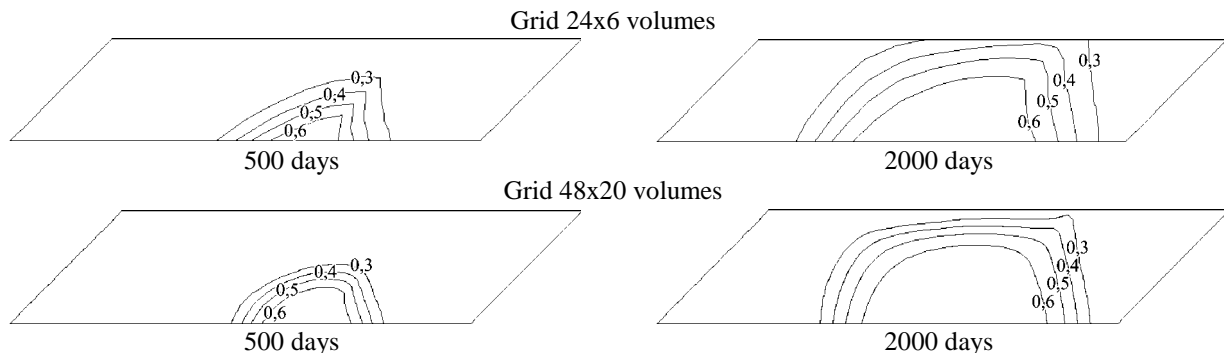
Figure 4 – Water saturation fields in two times.

The goal is to simulate the same problem using meshes with many levels of orthogonality. Initially the grid is cartesian, Fig. (5-a), i.e., it has a 90° inclination with a horizontal line. Other grids with 80°, 60°, 45°, 30° and 20° inclinations were obtained distorting the original grid. As can be seen on Figure (5-b)-(5-f), for each case, the reservoir boundary was changed, but the distances from the injected to the producing wells were kept constant.
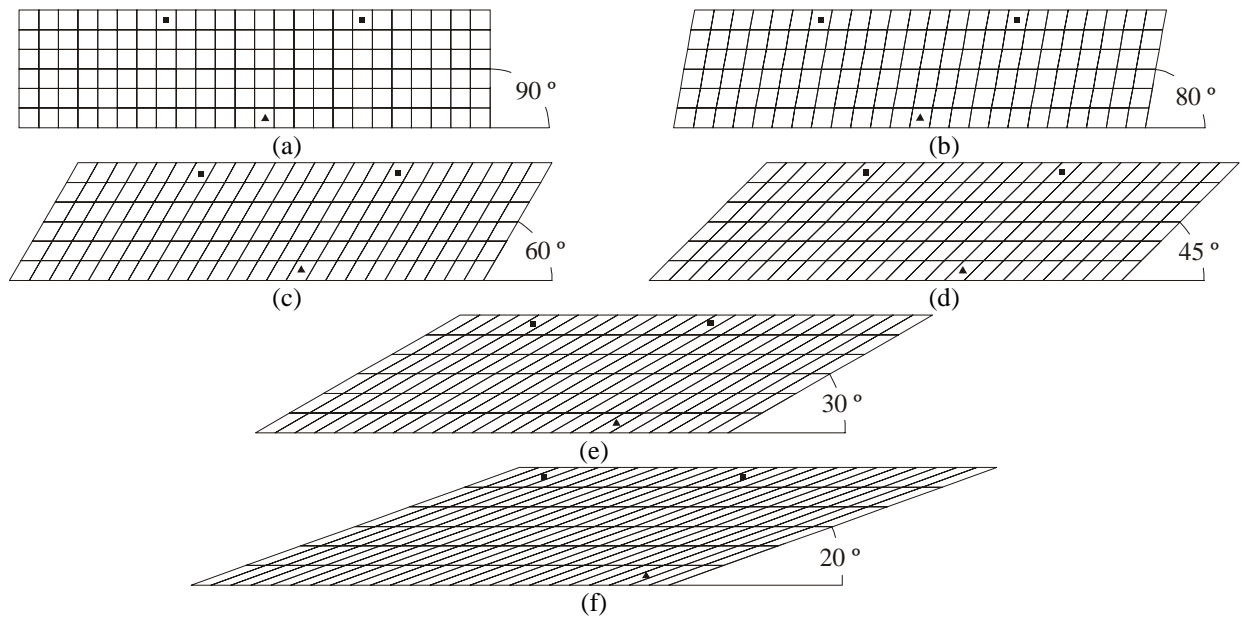
Figure 5 – Meshes with many levels of orthogonality.

Figure (6) shows many results obtained with simulations. Each plot contains curves generated using five and nine points schemes for both grids (24x6 and 48x20 volumes). On left column, the maximum time step used was 50 days, while on right one, 100 days. In all figures, the variables of vertical axis were evaluated from beginning till the end of simulation (7500 days). The meaning of each of these variables will be described next.

Figures (6-a) and (6-b) illustrate the number of time steps used with the maximum time step of 50 and 100 days, respectively. A greater quantity of increments means that the average time step used was small. From these figures, it can be noticed that the reduced Jacobian matrix (five-points) presents a great variation when angles equal to 60º or smaller were used. For small mesh angles, great variations occurred on mass fractions or pressures, that kept the average time step less than it was observed on orthogonal grid ($\theta = 90º$) or when the full Jacobian matrix (nine-points scheme) was used. It is also worth noticing that the maximum number of time steps increased when was used a more refined mesh.

The behavior of the number of time steps used was approximately linear for the full Jacobian matrix, but it was non-linear when it was used matrix including only direct neighboring volumes. The increase of the number of time steps with the number of volumes on the mesh can be explained by the increase of the mass fractions and pressure changes by time step. Finally, it can be mentioned that the number of time steps wasn't sensible to the grid orthogonality when using nine-points scheme. Five-points scheme required many time steps for skewed grids. Some tests couldn't be performed for determined grid angles, as seen on Figs. (6-a) and (6-b).

Figures (6-c) and (6-d) show the total number of necessary iterations to Newton's method convergence on each time step. As bigger the iterations number, greater will be computer costs to simulate. Note that, for both grids utilized, the two schemes presented the same efficiency only for 90º inclination mesh. In all other geometries, as skew angle increases, five-points scheme demand more Newton's method iterations. For full Jacobian matrix, the iterations number has small sensibility with growing mesh inclination and time step, for each skew angle.

Figures (6-e) and (6-f) present all solver iterations. Analyzing these figures, the number of solver iterations was not dependent on mesh inclination for full Jacobian matrix. It can be mentioned that, in the present work, the diagonal block as pre-conditioner matrix, which doesn't consider the complete structure of the Jacobian matrix was used. This pre-conditioner isn't extremely efficient such as an ILU pre-conditioner, according to (Marcondes et all, 1995 and Maliska et all, 1998), but it has been robust in all mesh inclinations analyzed. As for five-spot configuration, the iterations number varied with the growing of mesh angle.

Figures (6-g) and (6-h) show necessary time for composition of the Jacobian matrix and calculation of the residual functions. Note that, as greater the grid inclination, more time was wasted five-points scheme. As for full Jacobian matrix, this time haven't changed with variations on grid inclination. This fact could be explained with the increasing number of iterations of Newton's method with the grid angle to this matrix configuration, Figures (6-c) and (6-d). All simulations were made using a Silicon Graphics workstation - model Onyx 2.

Figures (6-i) and (6-j) exhibit the time consumed for solver to achieve the linear system solution. As commented in Figures (6-e) and (6-f), the solver iterations kept constant with the complete Jacobian matrix for all grid angles, then the solver time must maintain the same behavior. As for five-points scheme, the growth in the iterations number, as a function of mesh angle, doesn't increase necessarily the CPU time during simulation. This occurs due to operations done by BICGSTAB, proposed by Van Der Vorst (1992), such as matrix-vector product that require high computational cost. As greater the matrix structure, more expensive will be the computational process to the matrix-vector products. Comparing the number of solver iterations in Figure (6-c) for 60º skewed mesh (48x20), it can be seen that, using the

incomplete Jacobian matrix, approximately 5 times more iterations were needed. However, time wasted by solver is approximately the same for both schemes.
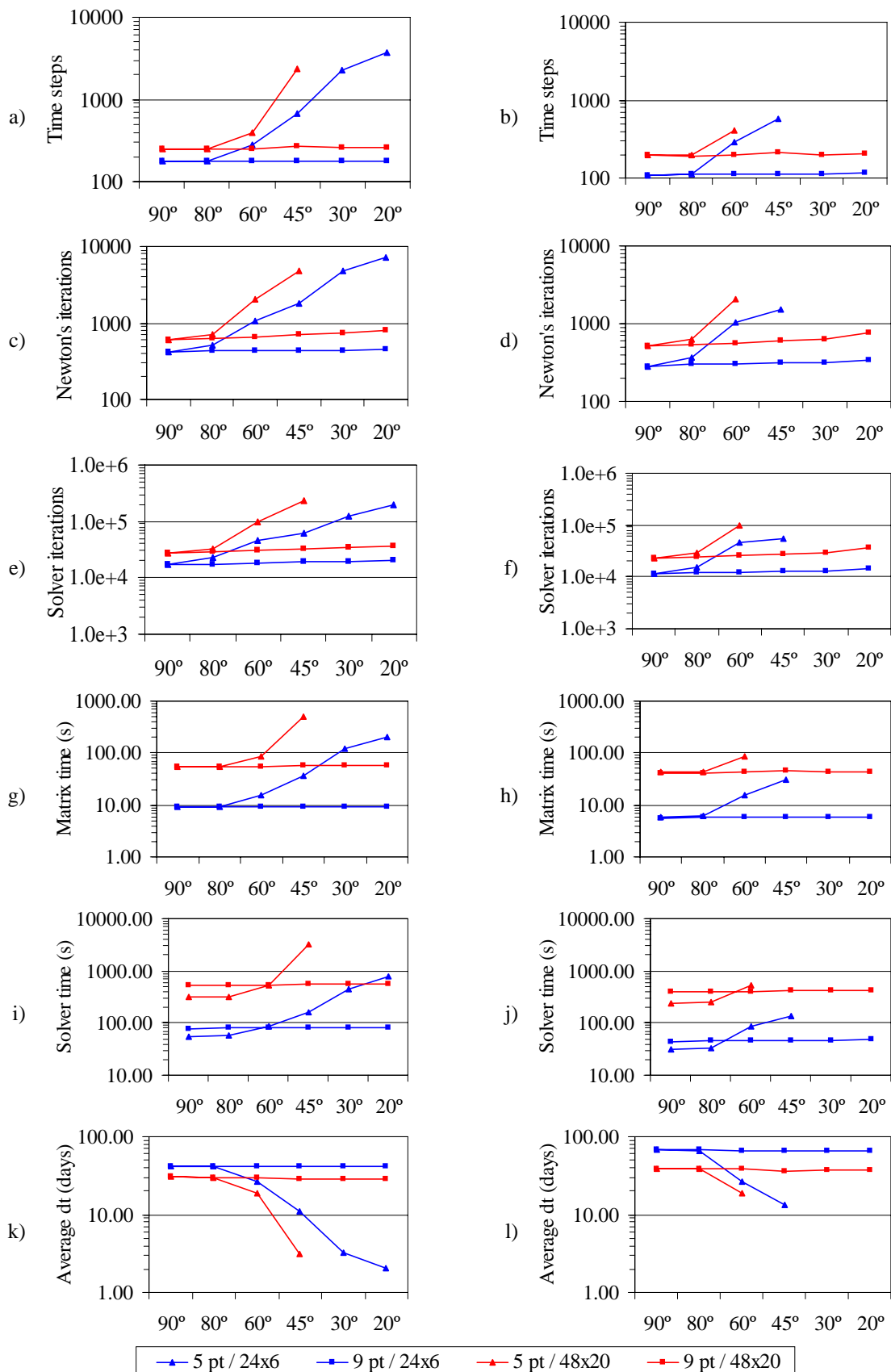
Figure 6 – Simulation results obtained with five-points and nine-points scheme.

Figures (6-k) and (6-l) illustrate average Δt used in the simulation. The smaller this value, the greater will be the total simulation time. Note that full Jacobian matrix presented a linear behavior, with high values of average Δt, as for incomplete matrix this value became lower for higher skew angles. Note that these curves have a similar behavior with those shown on Figures (6-a) and (6-b). This can be easily explained: as smaller the time steps during simulation, more of them will be needed to get total time.

To compare the results obtained with both schemes, Figs. 7 and 8 show water cut curves on producing wells 1 and 2 for grid with 24x6 and 48x20 control-volumes and 90º and 45º inclination with time step of 50 days. From this figures, it is possible to notice that results achieved with five-points and nine-points schemes are very similar, with small differences, only when it was used 45º inclination mesh. It is also possible to observe the grid orientation effects analyzing and comparing the time when water cut starts to increase.

(a) Producing well 1 (non-aligned)

(b) Producing well 2 (aligned)

Figure 7 – Water cut on 90º inclination grid, Δt =50 days.

(a) Producing well 1 (non-aligned)

(b) Producing well 2 (aligned)
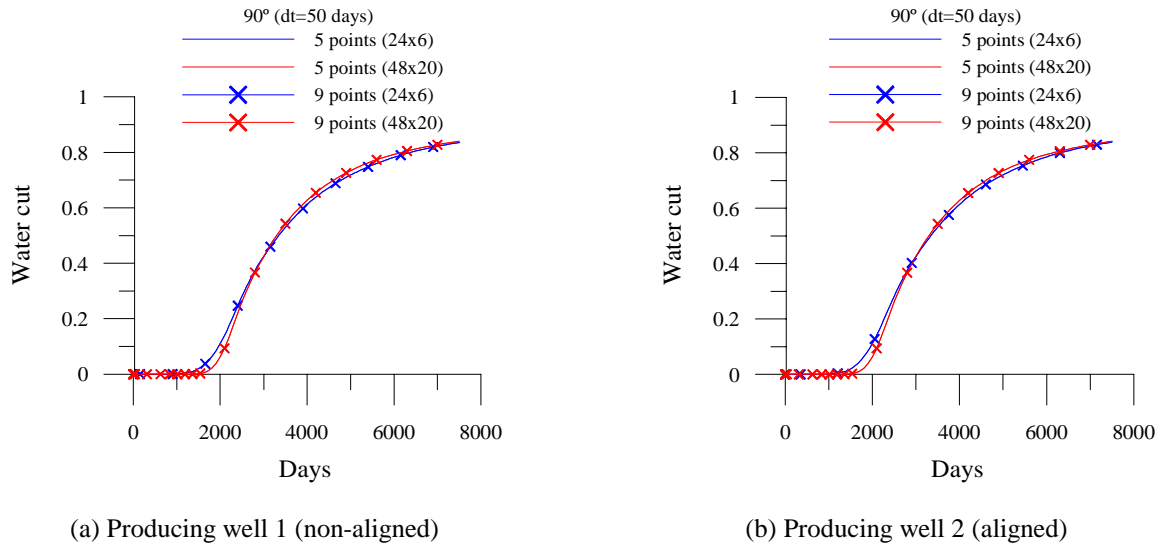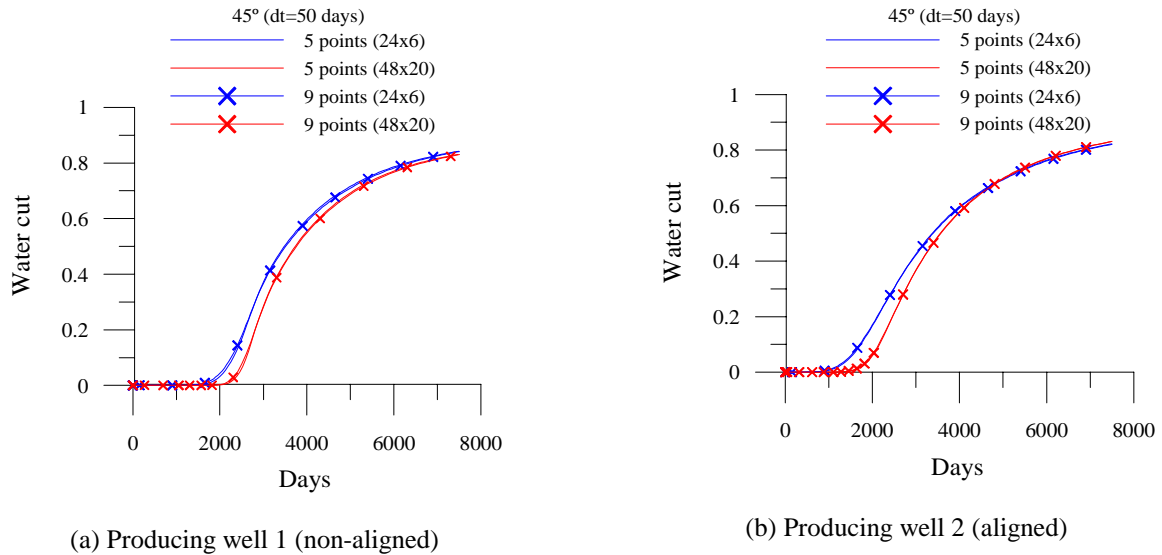
Figure 8 – Water cut on 45º inclination grid, Δt =50 days.

5. Conclusions

The efficiency of the five-points and nine-points schemes was tested in meshes with many levels of orthogonality. It was observed that it is necessary take into account the cross terms during the construction of the Jacobian matrix for meshes with high levels of non-orthogonality. Although this fact may contribute to increase CPU time (in each solver iteration), there is a substantial reduction on the number of Newton's method iterations and in the number of time steps employed. The use of full Jacobian matrix allows using large time steps in all simulations.

6. Acknowledgement

7. References

Coutinho, B. G., 2002, "Numerical Solution for Problems of Petroleum Reservoirs Using Generalized Coordinates", Msc Dissertation, Federal University of Campina Grande, Brazil. (In Portuguese)

Cunha, A. R., 1996, "A Metodology to Three Dimensional Numerical Simulation of Petroleum Reservoirs Using Black-Oil Model and Mass Fraction Formulation", Msc Dissertation, Federal University of Santa Catarina, Brazil. (In Portuguese)

Cunha, A. R., Maliska, C. R., Silva, A. F. C. e Livramento, M. A., 1994, "Two-Dimensional Two-Phase Petroleum Reservoir Simulation Using Boundary-Fitted Grids", RBCM, Vol. XVI, no. 4, pp. 423-429.

Czesnat, A. O., Maliska, C. R., Silva, A. F. C., Lucianetti, R. M., 1998, "Grid Effects on petroleum reservoir simulation using boundary-fitted generalized coordinates", VII ENCIT, Rio de Janeiro, Brazil. (In Portuguese)

Hegre, T. M., Dalen V. And Henriquez, A., 1986, "Generalized Transmissibilities For Distorted Grids in Reservoir Simulation", SPE 15622, October.

Hirasaki, G. J. e O'Dell, P. M., 1970, "Representation of Reservoir Geometry for Numerical Simulation", SPEJ.

Marcondes, F., 1996, "Numerical Simulation Using Implicit-Adaptative Mehotds and Voronoi Meshs in Problems of Petroleum Reservoirs." Dr Thesis, Departament of Mechanical Engineering, Federal University of Santa Catarina, Brazil. (In Portuguese)

Maliska, C. R., 1995, "Computational Heat Transfer and Fluid Mechanics", LTC, Rio de Janeiro, Brazil. (In Portuguese)

Prais, F. e Campagnolo, E. A., 1991, "Multiphase Flow Modeling in Reservoir Simulation". Anais XI COBEM, São Paulo, SP.

Todd, M. R., O´Dell, P. M. E Hirasaki, G. T., 1972, "Methods for Increasing Accuracy in Numerical Reservoir Simulators", SPEJ.

Van Der Vorst, H. A., 1992, "BI-CGSTAB: A Fast and Smoothly Converging Variant of Bi-CG for the Solution of Nonsymmetric Linear Systems. SIAM J. SCI. STAT. COMPUT., 13(2):631-644.

8. Copyright Notice